Organometallics 1992, *11*, 1334–1342

Solution and Solid-State Structures of Several Dialkyltin Dicarboxylate Complexes, $[R_2Sn(O_2CR'CO_2)]_x$: Polymorphic Organotin Polymers

Jeffrey H. Wengrovius* and Mary F. Garbauskas

GE Research & Development, P.O. Box 8, Schenectady, New York 12301

Received May 10, 1991

Single-crystal X-ray structures of three crystalline phases of $[\mathrm{Bu_2Sn(diethylmalonato)}]_x$ (1, phases I–III, $[\mathrm{Bu_2Sn(O_2CCEt_2CO_2)}]_x$) and the diamine complex $[\mathrm{Bu_2Sn(diethylmalonato)}((\gamma\text{-}((\mathrm{aminoethyl})\mathrm{amino})\mathrm{propyl})\mathrm{trimethoxysilane})]_x$ (2; $[\mathrm{Bu_2Sn(O_2CCEt_2CO_2)(H_2N(CH_2)_2NH(CH_2)_3Si(OMe)_3)}]_x$) are reported and compared with structures of dialkyltin bis(monocarboxylate) derivatives. In the solid state, these molecules are linear polymers with dicarboxylate groups bridging Sn atoms. The three polymorphs of $[\mathrm{Bu_2Sn(diethylmalonato)}]_x$ exhibit structures with subtle differences in the bond lengths and angles between the tin atoms and the oxygen atoms of the anisobidentate carboxylate groups. In solution these and other dialkyltin complexes of dicarboxylic acids adopt oligomeric, cyclic structures as determined by ^{119}Sn NMR, IR, and molecular weight analyses. The solubility of $[\mathrm{Bu_2Sn(dicarboxylato)}]_x$ compounds is facilitated by rapid intermolecular carboxylate-exchange reactions. Crystal data for 1, phase I: monclinic, $P2_1/c$, $a = 12.897$ (6) Å, $b = 10.530$ (5) Å, $c = 13.52$ (1) Å, $\beta = 108.38$ (5)°, $V = 1742.5$ Å^3, $Z = 4$, $R = 0.0314$ for 1991 unique reflections. Crystal data for 1, phase II: monoclinic, $P2_1/n$, $a = 11.342$ (2) Å, $b = 11.677$ (3) Å, $c = 13.535$ (4) Å, $\beta = 108.64$ (2)°, $V = 1698.6$ Å^3, $Z = 4$, $R = 0.0529$ for 2327 unique reflections. Crystal data for 1, phase III: monoclinic, $P2_1$, $a = 12.062$ (6) Å, $b = 11.188$ (7) Å, $c = 14.597$ (6) Å, $\beta = 114.38$ (2)°, $V = 1794.2$ Å^3, $Z = 2$, $R = 0.0996$ for 1417 unique reflections. Crystal data for 2: monoclinic, $P2_1/a$, $a = 13.59$ (1) Å, $b = 13.06$ (1) Å, $c = 17.74$ (2) Å, $\beta = 106.15$ (8)°, $V = 3024.8$ Å^3, $Z = 4$, $R = 0.0560$ for 3417 unique reflections.

Introduction

Diorganotin dicarboxylate complexes are industrially important as PVC stabilizers[1] and as catalysts for transesterification reactions,[2] polyurethane polymerizations,[2] and RTV silicone curing reactions.[3] Several diorganotin(IV) derivatives also exhibit antitumor properties.[4] Although the solution[5] and solid-state[5b,6] structures of diorganotin dicarboxylate compounds derived from monocarboxylic acids ($R_2Sn(O_2CR')_2$) have been reported, the structures of the related complexes derived from dicarboxylic acids ($[R_2Sn(O_2CR'CO_2)]_x$) are poorly understood.

The first literature reference to dibutyltin dicarboxylates prepared from dicarboxylic acids[7] presents evidence supporting cyclic oligomeric structures in solution (structure a). Linear polymeric structures (structure b) are proposed as the products of interfacial polymerization of Bu_2SnCl_2 and dicarboxylic acids,[8] and more recently monomeric structures containing intramolecular dicarboxylate ligands (structure c) have been suggested.[9] Structures a–c are drawn with monodentate carboxylate groups (Sn coordination number of 4). It is well-known that carboxylate groups often bond to Sn atoms in a bidentate fashion, and thus, variations of structures a–c with higher coordination numbers are possible. The goal of our research is to more clearly understand the mode of bonding in this class of compounds.

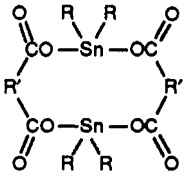

a

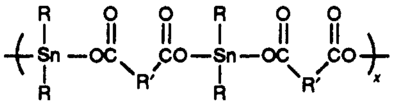

b

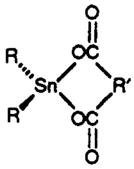

c

In this paper we report the X-ray structures of three crystalline polymorphs of the organometallic polymer, $[\mathrm{Bu_2Sn(diethylmalonato)}]_x$ (1). The importance of intermolecular carboxylate-exchange reactions on the solution structures of this and related compounds is also discussed. In addition, the polymeric structure of a diamine complex of 1 is presented.

Results and Discussion

Synthesis and Molecular Structures of $[Bu_2Sn(O_2CCEt_2CO_2)]_x$. We have previously reported the synthesis of 1 from $Bu_2Sn(O)$ and diethylmalonic acid in toluene.[10] This crystalline compound is soluble in hot toluene and recrystallizes on cooling. However, X-ray diffraction powder patterns of various samples of this product showed differences depending on the rate of crystallization. Crystals of three different crystalline

---

(1) Davis, A. G.; Smith, P. J. In *Comprehensive Organometallic Chemistry*; Stone, F. G. A.; Abel, E. W., Eds.; Pergamon: New York, 1982; Vol. 2, pp 610–616 (see also references cited therein).

(2) Evans, C. J.; Karpel, S. *J. Organomet. Chem. Libr.* 1985, *16*, 1.

(3) Gross, D. C. *Inorg. Chem.* 1989, *28*, 2355.

(4) Crowe, A. J. *Drugs Future* 1987, *12*, 255.

(5) (a) Lockhart, T. P.; Manders, W. F.; Holt, E. M. *J. Am. Chem. Soc.* 1986, *108*, 6611. (b) Chandrasekhar, V.; Day, R. O.; Holmes, J. M.; Holmes, R. R. *Inorg. Chem.* 1988, *27*, 958.

(6) Lockhart, T. P.; Calabrese, J. C.; Davidson, F. *Organometallics* 1987, *6*, 2479.

(7) Andrews, T. M.; Bower, F. A.; LaLiberte, B. R.; Montermoso, J. C. *J. Am. Chem. Soc.* 1958, *80*, 4102.

(8) Carraher, C. E.; Dammeier, R. L. *J. Polym. Sci., Part A-1* 1972, *10*, 413.

(9) Gielen, M.; Melotte, M.; Atassi, G.; Willem, R. *Tetrahedron* 1989, *45*, 1219.

(10) Wengrovius, J. H.; Lockhart, T. P. U.S. Patent 4,667,007, May 19, 1987 (assigned to the General Electric Co.).

0276-7333/92/2311-1334$03.00/0

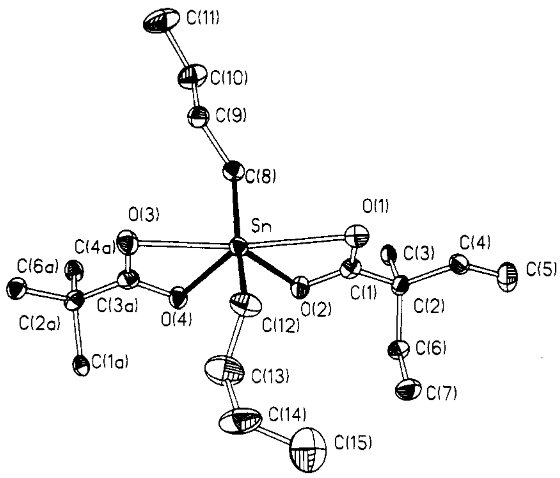

Figure 1. Thermal ellipsoid (50%) plot of phase I of 1. Figures 1–3 are drawn to emphasize the bicapped tetrahedral structure of phases I–III.

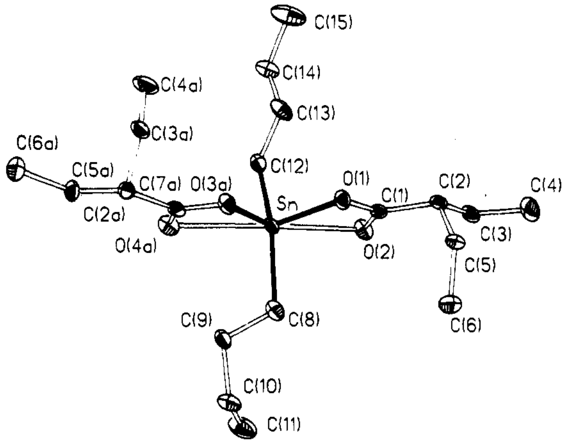

Figure 2. Thermal ellipsoid (50%) plot of phase II of 1.

Table I. Atomic Coordinates (×10⁴) and Equivalent Isotropic Displacement Coefficients (Å² × 10³) for Phase I

	x	*y*	*z*	*U*(eq)[a]
Sn	4491 (1)	3735 (1)	−1400 (1)	19 (1)
O(1)	5956 (3)	5434 (3)	−371 (2)	25 (1)
O(2)	5795 (3)	4507 (3)	−1874 (2)	25 (1)
O(3)	7011 (3)	7192 (3)	−2970 (3)	28 (1)
O(4)	5767 (3)	7600 (3)	−2213 (2)	23 (1)
C(1)	6266 (4)	5328 (4)	−1155 (3)	21 (2)
C(2)	7181 (4)	6130 (4)	−1326 (4)	22 (2)
C(3)	6638 (4)	6996 (4)	−2238 (3)	22 (2)
C(4)	7721 (4)	6968 (5)	−363 (3)	24 (2)
C(5)	8612 (5)	7844 (5)	−497 (4)	39 (2)
C(6)	7998 (4)	5242 (5)	−1601 (4)	24 (2)
C(7)	8563 (4)	4289 (5)	−743 (4)	34 (2)
C(8)	3392 (4)	5215 (5)	−2094 (4)	23 (2)
C(9)	2267 (4)	5290 (5)	−1935 (4)	26 (2)
C(10)	1527 (4)	6253 (6)	−2648 (4)	38 (2)
C(11)	448 (5)	6397 (6)	−2442 (5)	52 (3)
C(12)	5357 (5)	2403 (5)	−251 (4)	32 (2)
C(13)	5845 (6)	1351 (6)	−697 (5)	54 (3)
C(14)	6626 (5)	530 (6)	170 (5)	54 (3)
C(15)	7774 (6)	981 (7)	629 (5)	64 (3)

[a] Equivalent isotropic *U* defined as one-third of the trace of the orthogonalized U_{ij} tensor.

Table II. Atomic Coordinates (×10⁴) and Equivalent Isotropic Displacement Coefficients (Å² × 10³) for Phase II

	x	*y*	*z*	*U*(eq)[a]
Sn	1689 (1)	1070 (1)	1183 (1)	16 (1)
O(1)	1676 (5)	−24 (4)	2452 (4)	20 (2)
O(2)	226 (5)	−589 (5)	1026 (4)	22 (2)
O(3)	1883 (5)	−3050 (4)	2650 (4)	20 (2)
O(4)	2009 (5)	−2266 (5)	4168 (4)	24 (2)
C(1)	760 (7)	−707 (6)	1973 (6)	16 (2)
C(2)	366 (7)	−1597 (6)	2636 (6)	19 (2)
C(3)	−652 (7)	−2379 (6)	1919 (6)	22 (3)
C(4)	−1154 (8)	−3250 (7)	2493 (7)	33 (3)
C(5)	−80 (7)	−934 (6)	3441 (6)	23 (3)
C(6)	−1254 (8)	−215 (7)	2956 (7)	29 (3)
C(7)	1501 (7)	−2329 (6)	3217 (6)	21 (3)
C(8)	137 (8)	2143 (7)	1013 (6)	25 (3)
C(9)	407 (7)	3428 (6)	1010 (6)	22 (3)
C(10)	−736 (8)	4163 (7)	984 (7)	26 (3)
C(11)	−1846 (9)	4048 (8)	−7 (9)	44 (4)
C(12)	2654 (7)	86 (7)	365 (6)	20 (2)
C(13)	3505 (8)	−851 (6)	1042 (6)	27 (3)
C(14)	4244 (8)	−1468 (7)	450 (7)	32 (3)
C(15)	5122 (11)	−2386 (9)	1102 (8)	51 (4)

[a] Equivalent isotropic *U* defined as one-third of the trace of the orthogonalized U_{ij} tensor.

Table III. Atomic Coordinates (×10⁴) and Equivalent Isotropic Displacement Coefficients (Å² × 10³) for Phase III

	x	*y*	*z*	*U*(eq)[a]
Sn(1)	−627 (3)	1526	3682 (3)	56 (1)
Sn(2)	451 (4)	3827 (4)	1257 (5)	102 (3)
O(1)	658 (27)	2523 (28)	4930 (22)	54 (9)
O(2)	837 (27)	3228 (27)	3517 (25)	44 (8)
O(3)	2286 (47)	5001 (47)	6579 (41)	126 (18)
O(4)	833 (28)	5561 (28)	5174 (24)	48 (8)
O(5)	978 (57)	4849 (57)	169 (50)	141 (23)
O(6)	2018 (31)	5511 (32)	1631 (27)	70 (10)
O(7)	943 (56)	7328 (58)	−1421 (48)	170 (24)
O(8)	938 (43)	7908 (49)	−73 (38)	117 (19)
C(1)	965 (57)	3180 (60)	4142 (53)	91 (21)
C(2)	2101 (43)	4046 (45)	5171 (36)	56 (13)
C(3)	2681 (57)	4787 (61)	4396 (50)	92 (20)
C(4)	3507 (62)	5648 (63)	5073 (51)	133 (28)
C(5)	2914 (61)	3522 (66)	5774 (53)	128 (25)
C(6)	3591 (64)	2510 (69)	5225 (53)	144 (29)
C(7)	1598 (45)	4820 (44)	5684 (39)	50 (13)
C(8)	311 (39)	351 (36)	3247 (32)	51 (11)
C(9)	851 (58)	−1015 (67)	3571 (49)	133 (24)
C(10)	1588 (74)	−1410 (85)	2933 (72)	165 (34)
C(11)	2801 (68)	−1200 (81)	3366 (61)	197 (37)
C(12)	−1911 (77)	2677 (79)	3031 (59)	152 (36)
C(13)	−2259 (82)	3495 (93)	3805 (65)	223 (47)
C(14)	−3478 (79)	4473 (98)	3136 (75)	219 (45)
C(15)	−4342 (110)	4085 (126)	1913 (91)	659 (164)
C(16)	1732 (64)	5333 (68)	751 (58)	103 (22)
C(17)	2370 (52)	6287 (58)	67 (42)	93 (21)
C(18)	3383 (44)	7206 (43)	962 (37)	72 (14)
C(19)	4089 (50)	8021 (52)	596 (44)	93 (18)
C(20)	2671 (73)	5686 (81)	−503 (65)	128 (31)
C(21)	4024 (42)	4851 (42)	54 (37)	71 (14)
C(22)	1333 (38)	7160 (37)	−439 (33)	42 (10)
C(23)	1980 (58)	2465 (60)	1825 (44)	92 (19)
C(24)	2665 (68)	2088 (68)	1615 (55)	137 (26)
C(25)	3752 (73)	1211 (82)	1758 (66)	129 (33)
C(26)	4431 (50)	1122 (52)	1466 (44)	109 (21)
C(27)	−1213 (86)	5257 (88)	1124 (75)	215 (44)
C(28)	−613 (82)	5470 (90)	2129 (71)	206 (47)
C(29)	−1435 (93)	6941 (133)	2507 (73)	354 (75)
C(30)	−2217 (52)	7029 (52)	1343 (39)	112 (20)

[a] Equivalent isotropic *U* defined as one-third of the trace of the orthogonalized U_{ij} tensor.

phases of 1 (phases I–III) were subsequently isolated and their molecular structure determined by single crystal X-ray diffraction. The low temperature (−100 °C) structures of phases I and II refined well. However, crystals of phase III fractured on cooling to −100 °C, and thus the structure had to be determined at room temperature and contains some residual thermal motion associated with most of the carbon atoms. Despite the high *R* value, the coordination geometry about the Sn atoms was sufficiently determined to permit comparisons with phases I and II.

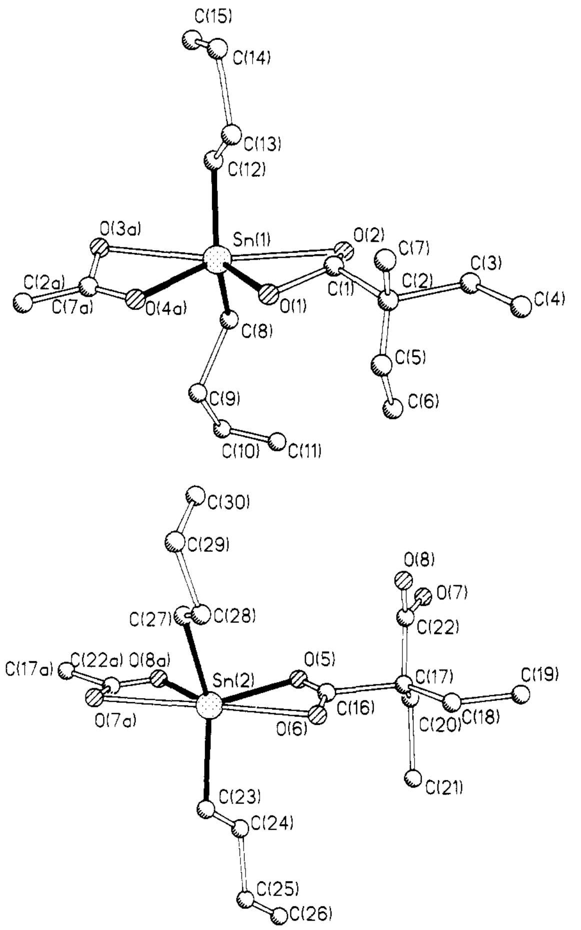

Figure 3. Ball and stick plots of both unique molecules of phase III of 1.

Table IV. Selected Bond Lengths (Å) for 1

	Phase I		
Sn–O(1)	2.655 (6)	Sn–O(2)	2.142 (6)
Sn–O(3)	2.467 (6)	Sn–O(4)	2.160 (5)
Sn–C(8)	2.118 (6)	Sn–C(12)	2.129 (6)
O(1)–C(1)	1.249 (7)	O(2)–C(1)	1.297 (6)
O(3)–C(3)	1.245 (7)	O(4)–C(3)	1.301 (6)
	Phase II		
Sn–O(1)	2.145 (7)	Sn–O(2)	2.516 (7)
Sn–O(3a)	2.131 (6)	Sn–O(4a)	2.576 (8)
Sn–C(8)	2.115 (9)	Sn–C(12)	2.123 (9)
O(1)–C(1)	1.298 (8)	O(2)–C(1)	1.241 (9)
O(3)–C(7)	1.307 (10)	O(4)–C(7)	1.226 (9)
	Phase III		
Sn(1)–O(1)	2.152 (27)	Sn(1)–O(2)	2.674 (35)
Sn(1)–O(3a)	2.536 (55)	Sn(1)–O(4a)	2.089 (37)
Sn(1)–C(8)	2.001 (50)	Sn(1)–C(12)	1.934 (83)
Sn(2)–O(5)	2.253 (78)	Sn(2)–O(6)	2.563 (39)
Sn(2)–O(7a)	2.454 (72)	Sn(2)–O(8a)	2.112 (45)
Sn(2)–C(23)	2.269 (65)	Sn(2)–C(27)	2.510 (104)
O(1)–C(1)	1.534 (89)	O(2)–C(1)	0.861 (68)
O(3)–C(7)	1.241 (68)	O(4)–C(7)	1.235 (54)
O(5)–C(16)	1.098 (85)	O(6)–C(16)	1.202 (91)
O(7)–C(22)	1.325 (80)	O(8)–C(22)	1.193 (77)

Table V. Selected Bond Angles (deg) for 1

	Phase I		
O(1)–Sn–O(2)	53.4 (2)	O(1)–Sn–O(3)	167.7 (2)
O(1)–Sn–O(4)	135.8 (2)	O(1)–Sn–C(8)	90.2 (2)
O(1)–Sn–C(12)	86.5 (2)	O(2)–Sn–O(3)	138.8 (2)
O(2)–Sn–O(4)	82.6 (2)	O(2)–Sn–C(8)	93.8 (2)
O(2)–Sn–C(12)	100.8 (2)	O(3)–Sn–O(4)	56.3 (2)
C(8)–Sn–O(3)	89.4 (2)	C(8)–Sn–O(4)	97.1 (2)
C(8)–Sn–C(12)	158.8 (2)	C(12)–Sn–O(3)	89.6 (2)
C(12)–Sn–O(4)	99.9 (2)		
	Phase II		
O(1)–Sn–O(2)	55.5 (2)	O(1)–Sn–O(3a)	83.8 (2)
O(1)–Sn–O(4a)	138.4 (2)	O(1)–Sn–C(8)	102.7 (3)
O(1)–Sn–C(12)	103.5 (3)	O(2)–Sn–O(3a)	139.3 (2)
O(2)–Sn–O(4a)	165.5 (2)	O(2)–Sn–C(8)	86.8 (3)
O(2)–Sn–C(12)	88.7 (3)	O(3a)–Sn–O(4a)	55.1 (2)
C(8)–Sn–O(3a)	101.7 (3)	C(8)–Sn–O(4a)	92.2 (3)
C(8)–Sn–C(12)	144.5 (3)	C(12)–Sn–O(3a)	104.6 (3)
C(12)–Sn–O(4a)	83.7 (3)		
	Phase III		
O(1)–Sn(1)–O(2)	55.7 (12)	O(1)–Sn(1)–O(3a)	136.4 (16)
O(1)–Sn(1)–O(4a)	82.7 (12)	O(1)–Sn(1)–C(8)	95.6 (22)
O(1)–Sn(1)–C(12)	102.8 (25)	O(2)–Sn(1)–O(3a)	167.1 (22)
O(2)–Sn(1)–O(4a)	137.8 (25)	O(2)–Sn(1)–C(8)	87.6 (15)
O(2)–Sn(1)–C(12)	84.7 (20)	O(3a)–Sn(1)–O(4a)	54.9 (15)
C(8)–Sn(1)–O(3a)	91.4 (19)	C(8)–Sn(1)–O(4a)	100.6 (16)
C(8)–Sn(1)–C(12)	136.4 (30)	C(12)–Sn(1)–O(3a)	87.2 (29)
C(12)–Sn(1)–O(4a)	113.7 (32)	O(5)–Sn(2)–O(6)	51.6 (12)
O(5)–Sn(2)–O(7a)	145.1 (21)	O(5)–Sn(2)–O(8a)	91.7 (22)
O(5)–Sn(2)–C(23)	100.1 (26)	O(5)–Sn(2)–C(27)	94.1 (32)
O(6)–Sn(2)–O(7a)	162.9 (21)	O(6)–Sn(2)–O(8a)	142.9 (22)
O(6)–Sn(2)–C(23)	90.0 (22)	O(6)–Sn(2)–C(27)	92.5 (22)
O(7a)–Sn(2)–O(8a)	53.4 (22)	C(23)–Sn(2)–O(7a)	89.5 (24)
C(23)–Sn(2)–O(8a)	102.9 (21)	C(23)–Sn(2)–C(27)	163.7 (32)
C(27)–Sn(2)–O(7a)	83.4 (29)	C(27)–Sn(2)–O(8a)	91.7 (22)

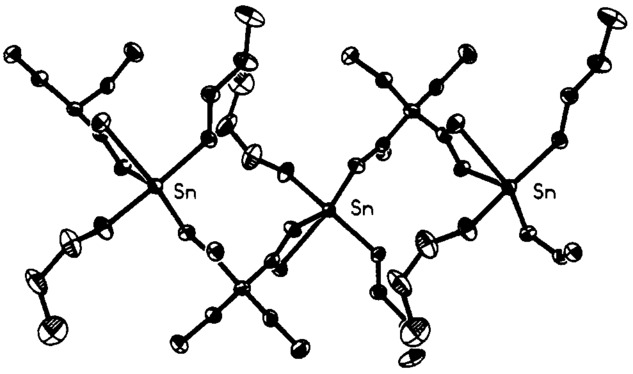

Figure 4. Extended structure of phase I of 1.

These structures are shown in Figures 1–3, and tables of atomic coordinates and bond lengths and angles are contained in Tables I–V.

Each of the crystal structures of 1 are polymers (structure b) comprised of Sn atoms linked together by dicarboxylate groups. These extended chains propagate throughout the crystal lattice by the symmetry elements of the space groups involved. The extended structure of phase I is shown in Figure 4. For phases I and II, there is only one unique molecule which propagates throughout the crystal. Phase III consists of two different molecules of 1 which propagate as independent alternating chains throughout the crystal lattice.

Each of the unique molecules in these structures are characterized by having 6-coordinate Sn atoms and anisobidentate carboxylate groups. The principle differences between the different polymorphs of 1 appear in the bond lengths and angles of the long and short Sn–O bonds of the carboxylate groups. In addition, the 6-coordinate arrangement of the oxygen and carbon atoms bound to Sn in these polymorphs is remarkably similar to those found in the structure of three dialkyltin dicarboxylate compounds derived from monocarboxylic acids, $\mathrm{Me_2Sn(O_2CMe)_2}$,[6] $\mathrm{Me_2Sn(O_2CC_6H_4\text{-}}p\mathrm{\text{-}NH_2)_2}$,[5b] and $\mathrm{Bu_2Sn}$(2,4,6-trimethylbenzoate)$_2$.[11]

Holmes and co-workers have described the structure of $\mathrm{Me_2Sn(O_2CC_6H_4\text{-}}p\mathrm{\text{-}NH_2)_2}$ as a bicapped tetrahedron.[5b]

---

[11] Garbauskas, M. F.; Wengrovius, J. H. *Acta Crystallogr.* **1991**, *C47*, 1969.

Table VI. Comparison of X-ray Structural Parameters between $[Bu_2Sn(O_2CRCO_2)]_x$ and $R_2Sn(O_2CR)_2$ Complexes

	short Sn–O bond lengths, Å	long Sn–O bond lengths, Å	max deviation out of SnO_4 plane, Å	"normal" tetrahedral bond angles, deg	distorted tetrahedral bond angles, deg	O–Sn–O bond angles between bicaps, deg
phase I of 1	2.160 (5), 2.142 (6)	2.467 (6), 2.655 (6)	0.04	93.8 (2)–100.8 (2)	82.6 (2), 158.8 (2)	167.7 (2)
phase II of 1	2.145 (7), 2.131 (6)	2.516 (7), 2.576 (8)	0.05	101.7 (3)–104.6 (3)	83.8 (2), 144.5 (3)	165.5 (2)
phase III of 1	2.152 (27), 2.089 (37)	2.536 (55), 2.674 (35)	0.05	95.6 (22)–113.7 (32)	82.7 (12), 136.4 (30)	167.1 (22)
	2.253 (78), 2.112 (45)	2.563 (39), 2.454 (72)	0.07	91.7 (22)–102.9 (21)	91.7 (22), 163.7 (32)	162.9 (21)
$Me_2Sn(O_2CMe)_2$[6]	2.106 (2)	2.539 (2)	0.07	105.7 (1)–107.8 (1)	79.5 (1), 135.9 (2)	170.3 (1)
Bu_2Sn(2,4,6-trimethylbenzoate)$_2$[11]	2.121 (12), 2.094 (13)	2.454 (14), 2.649 (14)	0.004	99.7 (4)–105.2 (4)	82.5 (3), 145.4 (5)	167.7 (3)
$Me_2Sn(O_2CC_6H_4\text{-}p\text{-}NH_2)_2$[5b]	2.077 (3), 2.097 (3)	2.556 (3), 2.543 (3)	0.094	104.2 (2)–110.5 (2)	81.8 (1), 134.7 (2)	168.0 (1)
compound 2	2.145 (6), 2.185 (6)	3.513 (9), 3.573 (9)	NA	NA	NA	NA

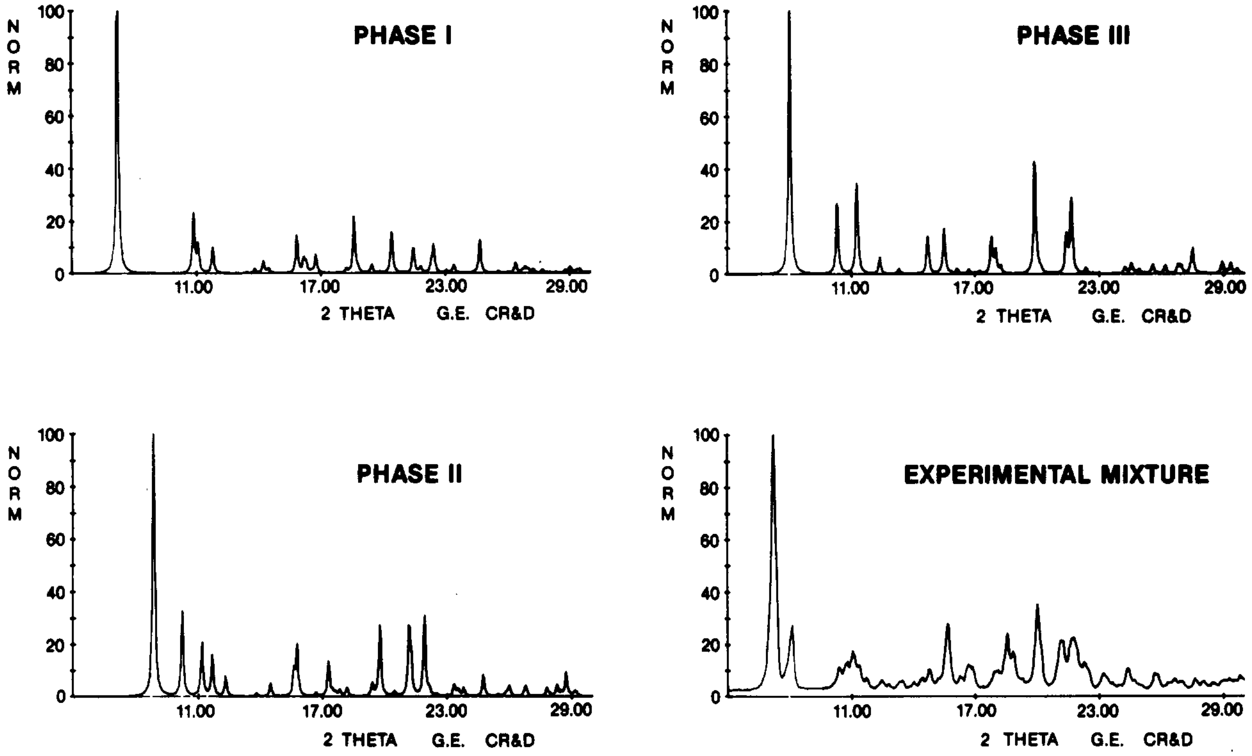

Figure 5. Simulated X-ray powder patterns of phases I–III of 1 and an actual X-ray powder pattern of a crystalline sample of 1.

Comparison of the structure of 1 with the three known structures of $R_2Sn(O_2CR')_2$ compounds indicates that all of these molecules are bicapped tetrahedra. The tetrahedra are formed by the two C atoms bonded to Sn and the two O atoms of the short Sn–O bonds. The tetrahedral bond angles of each phase of 1 consist of four relatively normal bond angles (102 ± 11°) and two bond angles distorted by the caps (87 ± 5 and 150 ± 14°). The O atoms of the long Sn–O bonds are the caps of the bicapped tetrahedra. The butyl groups are not trans; the Bu–Sn–Bu angles vary from 136.4 (30) to 163.7 (32)°. Also of note are the very large bond angles between the bicaps; O–Sn–O angles vary from 162.9 (21) to 167.7 (2)°. Figures 1–3 are drawn in a manner to allow easy comparison of the bicapped tetrahedral structures of phases I–III. Table VI highlights the structural similarities of these molecules and makes the appropriate comparisons with the other known $R_2Sn(O_2CR')_2$ structures.

All of these structures refined well enough to generate simulated X-ray powder patterns for each phase. Figure 5 shows an X-ray powder pattern of a recrystallized sample of compound 1 which, by comparison with powder patterns of each phase generated from the single-crystal data, is predominately phases I and III. By obtaining the X-ray powder patterns of several samples of 1, we demonstrated that one crystalline polymorph of 1 could be converted to the others depending on the conditions of recrystallization. This indicates that these phases easily interconvert in solution.

Synthesis and Molecular Structure of a Diamine Complex of $[Bu_2Sn(O_2CCEt_2CO_2)]_x$. Compound 1 is a Lewis acid and weakly coordinates amines in solution.[12] We isolated a diamine complex of 1 (2) with (γ-((aminoethyl)amino)propyl)trimethoxysilane ($H_2N(CH_2)_2NH(CH_2)_3Si(OMe)_3$). This diamine is a commonly used ad-

---

(12) Some base adducts of $[Bu_2Sn(\text{dicarboxylato})]_x$ complexes with dimethyl sulfoxide, pyridine *N*-oxide, pyridine, and picoline have been reported: Narula, S. P.; Sharma, R. K.; Lata, S.; Kapur, N.; Seth, R. *Ind. J. Chem.* **1983**, *22A*, 248.

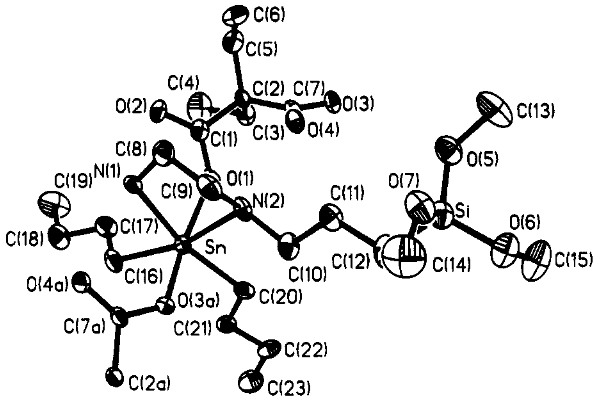

Figure 6. Thermal ellipsoid (50%) plot of 2.

Table VII. Atomic Coordinates ($\times 10^4$) and Equivalent Isotropic Displacement Coefficients ($Å^2 \times 10^3$) for 2

	x	*y*	*z*	*U*(eq)[a]
Sn	1178 (1)	−2573 (1)	1905 (1)	20 (1)
Si	−1403 (2)	1211 (2)	3924 (1)	35 (1)
O(1)	−11 (3)	−3644 (4)	1926 (3)	25 (2)
O(2)	656 (4)	−4898 (4)	2783 (3)	33 (2)
O(3)	−2736 (3)	−3699 (4)	2186 (3)	26 (2)
O(4)	−1272 (4)	−2997 (4)	2918 (3)	27 (2)
O(5)	−2080 (4)	292 (4)	4141 (3)	40 (2)
O(6)	−2096 (4)	2248 (4)	3672 (3)	49 (2)
O(7)	−506 (4)	1495 (5)	4719 (3)	43 (2)
N(1)	2066 (4)	−3279 (5)	3075 (3)	25 (2)
N(2)	546 (4)	−1769 (5)	2891 (3)	23 (2)
C(1)	−75 (6)	−4403 (6)	2380 (4)	25 (3)
C(2)	−1193 (5)	−4661 (6)	2350 (4)	23 (3)
C(3)	−1706 (6)	−5098 (6)	1521 (5)	34 (3)
C(4)	−1162 (7)	−6031 (7)	1297 (6)	57 (4)
C(5)	−1281 (7)	−5457 (7)	2969 (6)	42 (4)
C(6)	−929 (7)	−5089 (7)	3819 (5)	52 (4)
C(7)	−1749 (5)	−3695 (6)	2492 (4)	22 (3)
C(8)	1731 (7)	−2927 (7)	3752 (5)	39 (3)
C(9)	1351 (6)	−1853 (7)	3652 (5)	33 (3)
C(10)	163 (7)	−703 (6)	2733 (5)	31 (3)
C(11)	−287 (6)	−286 (6)	3370 (4)	33 (3)
C(12)	−874 (7)	710 (7)	3137 (5)	41 (4)
C(13)	−2753 (7)	401 (8)	4626 (5)	59 (4)
C(14)	283 (7)	2210 (8)	4783 (6)	74 (5)
C(15)	−3009 (7)	2289 (8)	3024 (5)	64 (4)
C(16)	2131 (6)	−3491 (6)	1370 (4)	31 (3)
C(17)	1732 (6)	−4556 (6)	1117 (5)	33 (3)
C(18)	2451 (6)	−5206 (6)	788 (5)	39 (3)
C(19)	2034 (8)	−6266 (7)	541 (6)	62 (5)
C(20)	118 (5)	−1700 (6)	1021 (4)	27 (3)
C(21)	240 (5)	−1862 (6)	189 (4)	26 (3)
C(22)	−597 (6)	−1336 (6)	−455 (4)	29 (3)
C(23)	−433 (6)	−1461 (7)	−1270 (4)	44 (3)

[a] Equivalent isotropic *U* defined as one-third of the trace of the orthogonalized $\mathbf{U}_{ij}$ tensor.

Table VIII. Selected Bond Lengths (Å) and Angles (deg) for 2

Sn–O(1)	2.145 (6)	Sn–N(1)	2.284 (7)
Sn–N(2)	2.384 (8)	Sn–C(16)	2.168 (9)
Sn–C(20)	2.139 (8)	Sn–O(3a)	2.185 (6)
Si–O(5)	1.624 (7)	Si–O(6)	1.640 (7)
Si–O(7)	1.629 (6)	Si–C(12)	1.857 (10)
O(1)–C(1)	1.295 (9)	O(2)–C(1)	1.232 (9)
O(3)–C(7)	1.301 (8)	O(3)–Sna	2.185 (6)
O(4)–C(7)	1.245 (8)	O(5)–C(13)	1.427 (12)
O(6)–C(15)	1.438 (9)	O(7)–C(14)	1.407 (12)
N(1)–Ha	0.916 (49)	N(1)–C(8)	1.472 (12)
N(2)–C(9)	1.489 (9)	N(2)–C(10)	1.493 (10)
O(1)–Sn–N(1)	85.9 (2)	O(1)–Sn–N(2)	80.8 (2)
N(1)–Sn–N(2)	73.7 (2)	O(1)–Sn–C(16)	101.1 (3)
N(1)–Sn–C(16)	86.9 (3)	N(2)–Sn–C(16)	160.4 (2)
O(1)–Sn–C(20)	90.2 (3)	N(1)–Sn–C(20)	163.4 (3)
N(2)–Sn–C(20)	89.8 (3)	C(16)–Sn–C(20)	109.7 (3)
O(1)–Sn–O(3a)	162.8 (2)	N(1)–Sn–O(3a)	87.0 (2)
N(2)–Sn–O(3a)	82.2 (2)	C(16)–Sn–O(3a)	94.2 (3)
C(20)–Sn–O(3a)	92.2 (3)	O(5)–Si–O(6)	110.7 (3)
O(5)–Si–O(7)	107.5 (3)	O(6)–Si–O(7)	106.5 (3)
O(5)–Si–C(12)	106.4 (4)	O(6)–Si–C(12)	113.4 (4)
O(7)–Si–C(12)	112.2 (3)	Sn–O(1)–C(1)	133.9 (4)
C(7)–O(3)–Sna	130.1 (5)	Si–O(5)–C(13)	124.8 (6)
Si–O(6)–C(15)	123.6 (5)	Si–O(7)–C(14)	126.2 (5)
Sn–N(1)–Ha	104.5 (48)	Sn–N(1)–C(8)	114.3 (5)
Ha–N(1)–C(8)	113.1 (50)	Sn–N(2)–C(9)	108.1 (5)
Sn–N(2)–C(10)	116.8 (5)	C(9)–N(2)–C(10)	110.5 (6)
O(1)–C(1)–O(2)	125.2 (7)	O(3)–C(7)–O(4)	124.2 (7)
N(1)–C(8)–C(9)	111.6 (7)	N(2)–C(9)–C(8)	108.3 (6)
N(2)–C(10)–C(11)	113.2 (6)	Sn–C(20)–C(21)	113.5 (5)
Si–C(12)–C(11)	112.4 (6)	Sn–C(16)–C(17)	115.3 (5)

hesion promoter in silicone RTVs. Due to the high moisture sensitivity of 2, crystals were grown from hot toluene under argon. The low-temperature (−100 °C) single-crystal X-ray diffraction structure of 2 is shown in Figure 6; atomic coordinates and bond lengths and angles are listed in Tables VII and VIII. Like the structures of compound 1, 2 is a linear polymer in the solid state. One unique molecule propagates throughout the lattice. However, in this slightly distorted octahedral molecule, the butyl groups are cis (Bu–Sn–Bu angle is 109.7 (3)°) and the carboxylate groups are monodentate. The short Sn–O bond lengths are 2.185 (6) and 2.145 (6) Å, not unlike those in the three phases of 1. By contrast, the two nonbonding Sn–O distances are 3.513 (9) and 3.573 (9) Å. The Lewis acidity of the Sn atom is satisfied by the coordination of the diamine, thus lessening the interaction between Sn and the carbonyl oxygens of the carboxylate groups.

Preparation and Solution Characterization of Dialkyltin Complexes of Dicarboxylic Acids. We have synthesized a number of $[Bu_2Sn(dicarboxylato)]_x$ complexes by the reaction of $[Bu_2Sn(O)]_x$ with 1 equiv of dicarboxylic acid:[7]

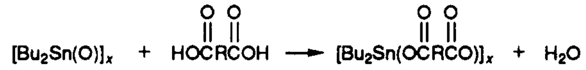

$$[Bu_2Sn(O)]_x + HO\overset{O}{\overset{\|}{C}}R\overset{O}{\overset{\|}{C}}OH \longrightarrow [Bu_2Sn(O\overset{O}{\overset{\|}{C}}R\overset{O}{\overset{\|}{C}}O)]_x + H_2O$$

R = CEt_2, CMe_2, $(CH_2)_2$, CH_2CMe_2, $(CH_2)_3$,
$CH_2CMe_2CH_2$, $(CH_2)_4$, $(CH_2)_8$, and C_6H_4 (phthalate)

All of these compounds are white crystalline solids and are soluble in solvents such as toluene and dichloromethane. These solubility characteristics are unusual since crystalline organometallic polymers having structures similar to 1 and 2 are typically insoluble in organic solvents. These observations suggest that these tin dicarboxylate derivatives are monomeric or oligomeric in solution. We have characterized a number of these compounds by ^1H NMR, ^{13}C NMR, ^{119}Sn NMR, and IR spectroscopy and by vapor-phase osmometry to determine molecular weight. Table IX summarizes the pertinent data.

The NMR spectra were clean and straightforward; for example, the ^{119}Sn NMR spectra showed sharp, single resonances between −40 and 25 °C for each tin dicarboxylate complex. The observed ^{119}Sn NMR shifts, −130 to −151 ppm, are in a range normally associated with 5-coordinate diorganotin compounds.[13] Examples of related 5-coordinate diorganotin compounds are the stannoxanes having the general formula $[R_2XSnOSnXR_2]_2$. These derivatives retain their solid structures in solution and typically have NMR shifts −150 to −250 ppm.[3,5b] By contrast, it is clear that the $[R_2Sn(dicarboxylato)]_x$ complexes reported in this paper do not retain their 6-coor-

---

[13] Harris, R. K.; Kennedy, J. D.; McFarlane, W. In *NMR and the Periodic Table*; Harris, R. K., Mann, B. E., Eds.; Academic Press: New York, 1978; pp 342–366.

Table IX. Solution Characterization Data for $[Bu_2Sn(dicarboxylato)]_x$ Compounds

compd	^{119}Sn NMR shift,[a] ppm	IR[c] ν_{CO} or ν_{OH}, cm^{-1}	mol wt[d]	x
$[Bu_2Sn(O_2CCMe_2CO_2)]_x$	−130	1610	1050	2.9
$[Bu_2Sn(O_2CCEt_2CO_2)]_x$	−131	1590	1100	2.8
$[Bu_2Sn(O_2C(CH_2)_2CO_2)]_x$	−147	1610	1950 (1430)[e]	5.6
$[Bu_2Sn(O_2CCH_2CMe_2CO_2)]^x$	−151	1600	1190	3.2
$[Bu_2Sn(O_2C(CH_2)_3CO_2)]_x$	−144	1600	2380	6.5
$[Bu_2Sn(O_2CCH_2CMe_2CH_2CO_2)]_x$	−148	1600	1750	4.5
$[Bu_2Sn(O_2C(CH_2)_4CO_2)]_x$	−146	1590	1520 (1205)[e]	4.0
$[Bu_2Sn(O_2C(CH_2)_8CO_2)]_x$	−150	1600	2250 (2950)[e]	5.2
$[Bu_2Sn(O_2CC_6H_4CO_2)]_x$	−138	1610	1090	2.7
$[Bu_2Sn(O_2CCEt_2CO_2)(AEAPTMS)]_x$[f]	−322[b]	1590	NA[g]	
$Bu_2Sn(O_2CCEt_2CO_2H)_2$	−132	3000, 1710, 1605	547 (551 calcd)	
$Bu_2Sn(O_2CCH_2CMeCO_2H)_2$	−151	3000, 1710, 1600	652 (523 calcd)	

[a] ^{119}Sn NMR spectra performed in $CDCl_3$ at +23 °C and referenced to Me_4Sn. [b] ^{119}Sn NMR spectra performed in CD_2Cl_2 at −80 °C. [c] Solution spectra in $CDCl_3$. [d] Vapor-phase osmometry in $CHCl_3$. [e] Values reported previously in ref 7. [f] AEAPTMS is (γ-((aminoethyl)amino)propyl)trimethoxysilane. [g] NA = not available.

dinate solid structures in solution. The typical solution IR spectrum exhibited a ν_{CO} stretch at 1590–1600 cm^{-1}. No bands associated with Sn–hydroxide end groups or with free carboxylic acid groups were detected.

The narrow range of NMR shifts and IR stretching frequencies suggests a common solution structure for these compounds. Since the solution molecular weight data indicated the presence of oligomers and the IR and NMR data showed the absence of end groups, the only plausible solution structure for these complexes is cyclic oligomers (structure a). Furthermore, since only one ^{119}Sn NMR resonance is observed for each of these compounds, we believe that several cyclic oligomers are in rapid equilibrium on the NMR time scale. We have no evidence for the formation of monomers containing intramolecular dicarboxylate groups (structure c). In fact, attempts at field desorption mass spectroscopy on several of these compounds did not yield monomeric molecular ions, only complex ions of higher molecular weight were observed.

^{119}Sn NMR spectroscopy of 2 showed that the diamine reversibly bonds to the Sn in solution. At 23 °C a broad resonance was observed at −256 ppm. Cooling to −80 °C or addition of more diamine, resulted in a sharper resonance at −322 ppm, which is in the chemical shift region normally associated with 6-coordinate diorganotin complexes.[13]

Solution Intermolecular Exchange Reactions. Our results indicate that dissolving 1 in dichloromethane requires a transformation from a linear, crystalline polymer to cyclic oligomers. This structural change requires intermolecular carboxylate group exchange reactions. Carboxylate group exchange was also implicated by ^{119}Sn NMR spectra of mixtures of $[Bu_2Sn(dicarboxylato)]_x$ complexes which showed averaged chemical shifts.

Another example of this reactivity is the reaction between 1 equiv of each $Bu_2Sn(O_2CMe)_2$ and 1. These compounds have widely separated individual ^{119}Sn NMR chemical shifts, −131 and −153 ppm, respectively. However, this mixture gave an averaged signal at −147 ppm due to the formation of a Sn dimer.

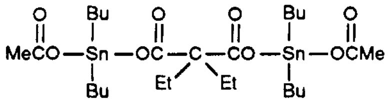

Attempts to isolate this dimer, however, gave back crystalline 1 and liquid $Bu_2Sn(O_2CMe)_2$, an indication of the reversibility of these exchange reactions.

Synthesis and Characterization of Bu_2Sn(dicarboxylato)$_2$ Complexes. Monomeric Bu_2Sn(dicarboxylato)$_2$ complexes were synthesized by the reaction of 2 equiv of a sterically hindered dicarboxylic acid with $[Bu_2Sn(O)]_x$:

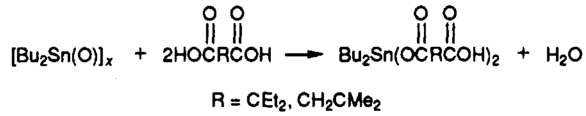

$$[Bu_2Sn(O)]_x + 2HO\overset{O}{\overset{\|}{C}}R\overset{O}{\overset{\|}{C}}OH \longrightarrow Bu_2Sn(O\overset{O}{\overset{\|}{C}}R\overset{O}{\overset{\|}{C}}OH)_2 + H_2O$$

$R = CEt_2, CH_2CMe_2$

These compounds can alternatively be prepared by reaction of an additional 1 equiv of dicarboxylic acid with 1 or $[Bu_2Sn$(1,1-dimethylsuccinato)$]_x$. We isolated white crystalline complexes whose ^1H NMR spectra verified the empirical formulas of Bu_2Sn(diethylmalonato)$_2$ (3) and Bu_2Sn(1,1-dimethylsuccinato)$_2$. Both compounds were monomeric in chloroform by vapor-phase osmometry. Their solution IR spectra showed a broad ν_{OH} band at 3000 cm^{-1} and two ν_{CO} stretches at 1710 and 1600 cm^{-1} assigned to the uncoordinated and coordinated portions of each dicarboxylate group, respectively. Attempts to prepare similar monomeric compounds containing adipate or phthalate groups were unsuccessful.

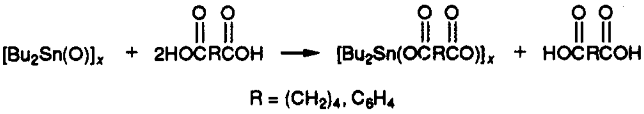

$$[Bu_2Sn(O)]_x + 2HO\overset{O}{\overset{\|}{C}}R\overset{O}{\overset{\|}{C}}OH \longrightarrow [Bu_2Sn(O\overset{O}{\overset{\|}{C}}R\overset{O}{\overset{\|}{C}}O)]_x + HO\overset{O}{\overset{\|}{C}}R\overset{O}{\overset{\|}{C}}OH$$

$R = (CH_2)_4, C_6H_4$

Compound 3 also exhibits rapid intermolecular carboxylate-exchange reactions in solution. The ^{13}C NMR spectrum of 3 showed only one averaged dicarboxylate carbonyl carbon until cooled to −80 °C, at which temperature this signal coalesced and the two expected carbonyl carbons appeared.

Conclusions

The observation that $[Bu_2Sn$(diethylmalonato)$]_x$ (1) is a crystalline organometallic polymer has helped us to understand why the properties of dialkyltin complexes of dicarboxylic acids are so different from those of the monomeric monocarboxylic acid derivatives ($R_2Sn(O_2CR)_2$). In general, the dicarboxylates are more crystalline, less soluble, and less moisture sensitive, have higher melting points, and decompose before boiling. Similarities between the properties of 1 and the other dicarboxylic acid tin complexes reported above allow us to predict that all of these compounds possess similar polymeric structures in the solid state.

The organotin polymers prepared by direct reaction of $[Bu_2Sn(O)]_x$ and dicarboxylic acids possess different structures than the tin polyesters synthesized interfacially by reaction of Bu_2SnCl_2 and dicarboxylic acids, as reported

Table X. Experimental Details of X-ray Structures

	phase I of 1	phase II of 1	phase III of 1	compd 2
lattice params				
no. of reflns	12	10	21	12
2θ range, deg	$9 \le 2\theta \le 21$	$7 \le 2\theta \le 18$	$4 \le 2\theta \le 17$	$7 \le 2\theta \le 18$
refln range				
h	0–14	0–14	0–15	0–17
k	0–12	0–14	0–14	0–17
l	−15 to +15	−17 to +17	−18 to +18	−22 to +22
max $(\sin\theta)/\lambda$	0.54	0.59	0.59	0.59
check reflections	$(0\bar{1}\bar{3})$, $(\bar{2}\bar{2}\bar{1})$	$(22\bar{1})$, $(2\bar{2}\bar{1})$	$(22\bar{1})$, (012)	$(\bar{2}0\bar{2})$, $(0\bar{1}3)$
% int variations	1 1	3 2	2 4	1 1
no. of reflns collcd	2451	3322	3512	5834
no. of unique reflns	1991	2327	1417	3417
obsd criterion	$F > 3\sigma(F)$	$F > 3\sigma(F)$	$F > 4\sigma(F)$	$F > 3\sigma(F)$
no. of params	181	181	170	310
R	0.0314	0.0529	0.0996	0.0560
R_w	0.0427	0.0772		0.0424
weighting factor, (g) $w - 1 = \sigma(F) + gFF$	0.0005	0.0044		0.00001
Fourier diff				
min, e/Å^3	−0.82	−2.45	−1.01	−0.83
max, e/Å^3	1.27	1.58	2.37	0.66
max shift/error	0.001	0.002	1.58	0.029

Table XI. ^{1}H NMR Spectroscopic Data

δ	mult	$^3J_{HH}$, Hz	int	assign
$[Bu_2Sn(O_2CCMe_2CO_2)]_x$				
1.71	m		4	SnC_1 and SnC_2
1.47	s		3	$O_2CC\mathit{Me}_2CO_2$
1.40	m		2	SnC_3
0.91	t	7.1	3	SnC_4
$[Bu_2Sn(O_2CCEt_2CO_2)]_x$				
1.98	q	7.4	2	$O_2CC(C\mathit{H}_2Me)_2CO_2$
1.72	m		4	SnC_1 and SnC_2
1.39	m		2	SnC_3
0.92	t	7.0	3	SnC_4
0.85	t	7.4	3	$O_2CC(CH_2\mathit{Me})_2CO_2$
$[Bu_2Sn(O_2C(CH_2)_2CO_2)]_x$				
2.67	s		2	$O_2C(C\mathit{H}_2)_2CO_2$
1.65	m		4	SnC_1 and SnC_2
1.37	m		2	SnC_3
0.91	t	7.3	3	SnC_4
$[Bu_2Sn(O_2CCH_2CMe_2CO_2)]_x$				
2.60	s		1	$O_2CC\mathit{H}_2CMe_2CO_2$
1.61	m		4	SnC_1 and SnC_2
1.33	m		2	SnC_3
1.27	s		3	$O_2CCH_2C\mathit{Me}_2CO_2$
0.87	t	7.3	3	SnC_4
$[Bu_2Sn(O_2C(CH_2)_3CO_2)]_x$				
2.49	t	7.3	2	$O_2CC\mathit{H}_2CH_2C\mathit{H}_2CO_2$
2.00	quin	7.3	1	$O_2CCH_2C\mathit{H}_2CH_2CO_2$
1.65	m		4	SnC_1 and SnC_2
1.36	m		2	SnC_3
0.92	t	7.0	3	SnC_4
$[Bu_2Sn(O_2CCH_2CMe_2CH_2CO_2)]_x$				
2.49	s		2	$O_2CC\mathit{H}_2CMe_2C\mathit{H}_2CO_2$
1.65	m		4	SnC_1 and SnC_2
1.38	h	7.3	2	SnC_3
1.17	s		3	$O_2CCH_2C\mathit{Me}_2CH_2CO_2$
0.90	t	7.3	3	SnC_4
$[Bu_2Sn(O_2C(CH_2)_4CO_2)]_x$				
2.38	t	4.8	2	$O_2CC\mathit{H}_2(CH_2)_2C\mathit{H}_2CO_2$
1.71	m		4	SnC_1 and SnC_2
1.66	t	3.3	2	$O_2CCH_2(C\mathit{H}_2)_2CH_2CO_2$
1.38	m		2	SnC_3
0.91	t	7.2	3	SnC_4
$[Bu_2Sn(O_2C(CH_2)_8CO_2)]_x$				
2.35	t	7.6	2	$O_2CC\mathit{H}_2(CH_2)_6C\mathit{H}_2CO_2$
1.64	m		6	SnC_1, SnC_2, and $O_2CCH_2C\mathit{H}_2(CH_2)_4C\mathit{H}_2CH_2CO_2$
1.37	h	7.3	2	SnC_3
1.31	bs		4	$O_2C(CH_2)_2(C\mathit{H}_2)_4(CH_2)CO_2$
0.91	t	7.3	3	SnC_4
$[Bu_2Sn(O_2CC_6H_4CO_2)]_x$				
7.75–7.49	AA′BB′		2	aromatic
1.92	t	8.2	2	SnC_1
1.72	m		2	SnC_2
1.28	h	7.3	2	SnC_3
0.80	t	7.3	3	SnC_4
$[Bu_2Sn(O_2CCEt_2CO_2)(H_2N(CH_2)_2NH(CH_2)_3Si(OMe)_3)]_x$				
3.53	s		9	$Si(O\mathit{Me})_3$
2.79	t	5.9	2	$NC\mathit{H}_2(CH_2)_2Si$
2.64	m		4	$H_2N(C\mathit{H}_2)_2N$
1.88	bm		4	$O_2CC(C\mathit{H}_2Me)_2CO_2$
1.59	m		10	SnC_1, SnC_2, and $NCH_2C\mathit{H}_2CH_2Si$
1.31	h	7.3	4	SnC_3
0.85	t	7.3	6	SnC_4
0.82	t	7.3	6	$O_2CC(CH_2\mathit{Me})_2CO_2$
0.61	t	8.3	2	$N(CH_2)_2C\mathit{H}_2Si$
				NH protons not located
$Bu_2Sn(O_2CCEt_2CO_2H)_2$				
10.85	bs		1	$O_2CCEt_2CO_2\mathit{H}$
1.97	q	7.3	4	$O_2C(C\mathit{H}_2Me)_2CO_2H$
1.69	m		4	SnC_1 and SnC_2
1.35	h	7.3	2	SnC_3
0.88	t	7.3	3	SnC_4
0.86	t	7.3	6	$O_2C(CH_2\mathit{Me})_2CO_2H$
$Bu_2Sn(O_2CCH_2CMe_2CO_2H)_2$				
11.02	bs		1	$O_2CCH_2CMe_2CO_2\mathit{H}$
2.66	s		2	$O_2CC\mathit{H}_2CMe_2CO_2H$
1.63	m		4	SnC_1 and SnC_2
1.37	h	7.3	2	SnC_3
1.31	s		6	$O_2CCH_2C\mathit{Me}_2CO_2H$
0.91	t	7.3	3	SnC4

by Carraher.[8] Tin polyesters prepared in this manner are generally less soluble and exhibit Sn–OH end groups.

The Lewis acidity of the Sn atoms in these complexes is important for catalytic applications.[2,3] The molecular structure of 2 and the polymorphic structures of 1 show that the acidity of the Sn can be satisfied either by reaction with a diamine or by intramolecular interactions with the carbonyl oxygens of the dicarboxylate groups. However, in solution these interactions are very dynamic as seen by rapid intermolecular carboxylate-exchange reactions.

Table XII. ^{13}C NMR Spectroscopic Data

δ	J_{CSn}, Hz	assgnt
		$\mathrm{[Bu_2Sn(O_2CCMe_2CO_2)]_{\mathit{x}}}$
183.0		$\mathrm{O_2\mathit{C}CMe_2\mathit{C}O_2}$
49.9		$\mathrm{O_2C\mathit{C}Me_2CO_2}$
26.6		$\mathrm{SnC_2}$
26.3		$\mathrm{SnC_3}$
25.1	528	$\mathrm{SnC_1}$
22.9		$\mathrm{O_2CC\mathit{Me}_2CO_2}$
13.4		$\mathrm{SnC_4}$
		$\mathrm{[Bu_2Sn(O_2CCEt_2CO_2)]_{\mathit{x}}}$
181.9		$\mathrm{O_2\mathit{C}CEt_2\mathit{C}O_2}$
58.6		$\mathrm{O_2C\mathit{C}Et_2CO_2}$
26.6		$\mathrm{SnC_2}$
26.3		$\mathrm{SnC_3}$
25.1	551	$\mathrm{SnC_1}$
23.9		$\mathrm{O_2CC(\mathit{C}H_2Me)_2CO_2}$
13.3		$\mathrm{SnC_4}$
8.5		$\mathrm{O_2CC(CH_2\mathit{Me})_2CO_2}$
		$\mathrm{[Bu_2Sn(O_2C(CH_2)_2CO_2)]_{\mathit{x}}}$
182.1		$\mathrm{O_2\mathit{C}(CH_2)_2\mathit{C}O_2}$
29.4		$\mathrm{O_2C(\mathit{C}H_2)_2CO_2}$
26.4		$\mathrm{SnC_2}$
26.2		$\mathrm{SnC_3}$
24.9	573	$\mathrm{SnC_1}$
13.4		$\mathrm{SnC_4}$
		$\mathrm{[(Bu_2Sn(O_2CCH_2CMe_2CO_2)]_{\mathit{x}}}$
187.4		$\mathrm{O_2CCH_2CMe_2\mathit{C}O_2}$
181.1		$\mathrm{O_2\mathit{C}CH_2CMe_2CO_2}$
44.2		$\mathrm{O_2CCH_2\mathit{C}Me_2CO_2}$
40.2		$\mathrm{O_2C\mathit{C}H_2CMe_2CO_2}$
26.5		$\mathrm{SnC_2}$
26.1		$\mathrm{SnC_3}$
25.4		$\mathrm{O_2CCH_2C\mathit{Me}_2CO_2}$
24.9	564, 594	$\mathrm{SnC_1}$
13.4		$\mathrm{SnC_4}$
		$\mathrm{[Bu_2Sn(O_2C(CH_2)_3CO_2)]_{\mathit{x}}}$
183.0		$\mathrm{O_2\mathit{C}(CH_2)_3\mathit{C}O_2}$
33.3		$\mathrm{O_2C\mathit{C}H_2CH_2\mathit{C}H_2CO_2}$
26.6		$\mathrm{SnC_2}$
26.2		$\mathrm{SnC_3}$
25.0	548, 578	$\mathrm{SnC_1}$
21.2		$\mathrm{O_2CCH_2\mathit{C}H_2CH_2CO_2}$
13.4		$\mathrm{SnC_4}$
		$\mathrm{[Bu_2Sn(O_2CCH_2CMe_2CH_2CO_2)]_{\mathit{x}}}$
182.3		$\mathrm{O_2\mathit{C}CH_2CMe_2CH_2\mathit{C}O_2}$
45.3		$\mathrm{O_2C\mathit{C}H_2CMe_2\mathit{C}H_2CO_2}$
32.3		$\mathrm{O_2CCH_2\mathit{C}Me_2CH_2CO_2}$
27.4		$\mathrm{O_2CCH_2C\mathit{Me}_2CH_2CO_2}$
26.7		$\mathrm{SnC_2}$
26.2		$\mathrm{SnC_3}$
25.1	573	$\mathrm{SnC_1}$
13.4		$\mathrm{SnC_4}$
		$\mathrm{[Bu_2Sn(O_2C(CH_2)_4CO_2)]_{\mathit{x}}}$
183.6		$\mathrm{O_2\mathit{C}(CH_2)_4\mathit{C}O_2}$
33.9		$\mathrm{O_2C\mathit{C}H_2(CH_2)_2\mathit{C}H_2CO_2}$
26.6		$\mathrm{SnC_2}$
26.2		$\mathrm{SnC_3}$
25.0	573	$\mathrm{SnC_1}$ and $\mathrm{O_2CCH_2(\mathit{C}H_2)_2CH_2CO_2}$
13.4		$\mathrm{SnC_4}$
		$\mathrm{[Bu_2Sn(O_2C(CH_2)_8CO_2)]_{\mathit{x}}}$
184.1		$\mathrm{O_2\mathit{C}(CH_2)_8\mathit{C}O_2}$
33.9		$\mathrm{O_2C\mathit{C}H_2(CH_2)_6\mathit{C}H_2CO_2}$
29.0, 28.9		$\mathrm{O_2CCH_2(\mathit{C}H_2)_2(CH_2)_2(\mathit{C}H_2)_2CH_2CO_2}$
26.5		$\mathrm{SnC_2}$
26.1		$\mathrm{SnC_3}$
25.3		$\mathrm{O_2C(CH_2)_3(\mathit{C}H_2)_2(CH_2)_3CO_2}$
24.7	560, 575	$\mathrm{SnC_1}$
13.4		$\mathrm{SnC_4}$
		$\mathrm{[Bu_2Sn(O_2CC_6H_4CO_2)]_{\mathit{x}}}$
177.4		$\mathrm{O_2\mathit{C}C_6H_4\mathit{C}O_2}$
132.4		$\mathrm{C_{\mathit{o}}}$
130.7		$\mathrm{C_{\mathit{m}}}$
129.0		$\mathrm{C_{\mathit{p}}}$
26.7		$\mathrm{SnC_2}$
26.2		$\mathrm{SnC_3}$
25.3	520, 558	$\mathrm{SnC_1}$
13.3		$\mathrm{SnC_4}$
		$\mathrm{[Bu_2Sn(O_2CCEt_2CO_2)(H_2N(CH_2)_2NH(CH_2)_3Si(OMe)_3)]_{\mathit{x}}}^{a}$
181.4		$\mathrm{O_2\mathit{C}CEt_2\mathit{C}O_2}$
59.2		$\mathrm{O_2C\mathit{C}Et_2CO_2}$
52.0		$\mathrm{H_2N(\mathit{C}H_2)_2N}$
50.5		$\mathrm{Si(O\mathit{Me})_3}$
40.9		$\mathrm{N\mathit{C}H_2(CH_2)_2Si}$
27.1		$\mathrm{NCH_2\mathit{C}H_2CH_2Si}$
26.6		$\mathrm{SnC_2}$
25.5		$\mathrm{SnC_3}$
25.1		$\mathrm{O_2CC(\mathit{C}H_2Me)_2CO_2}$
22.9		$\mathrm{SnC_1}$
13.6		$\mathrm{SnC_4}$
9.0		$\mathrm{O_2CC(CH_2\mathit{Me})_2CO_2}$
6.7		$\mathrm{N(CH_2)_2\mathit{C}H_2Si}$
		$\mathrm{Bu_2Sn(O_2CCEt_2CO_2H)_2}^{b}$
181, 179		$\mathrm{O_2\mathit{C}CEt_2\mathit{C}O_2H}$
57.6		$\mathrm{O_2C\mathit{C}Et_2CO_2H}$
26.3		$\mathrm{O_2CC(\mathit{C}H_2Me)_2CO_2H}$
25.5		$\mathrm{SnC_2}$
22.8		$\mathrm{SnC_3}$
18.8		$\mathrm{SnC_1}$
13.4		$\mathrm{SnC_4}$
7.8		$\mathrm{O_2CC(CH_2\mathit{Me})_2CO_2H}$
		$\mathrm{Bu_2Sn(O_2CCH_2CMe_2CO_2H)_2}$
187.3		$\mathrm{O_2CCH_2CMe_2\mathit{C}O_2H}$
181.2		$\mathrm{O_2\mathit{C}CH_2CMe_2CO_2H}$
44.5		$\mathrm{O_2CCH_2\mathit{C}Me_2CO_2H}$
40.4		$\mathrm{O_2C\mathit{C}H_2CMe_2CO_2H}$
26.7		$\mathrm{SnC_2}$
26.3		$\mathrm{SnC_3}$
25.8		$\mathrm{O_2CCH_2C\mathit{Me}_2CO_2H}$
25.3	563, 594	$\mathrm{SnC_1}$
13.5		$\mathrm{SnC_4}$

[a] ^{29}Si NMR δ-42. [b] NMR spectrum obtained at −80 °C in CD_2Cl_2.

The transformation from linear polymers in the crystal to cyclic oligomers in solution is driven by both thermodynamic and kinetic factors. The rapid kinetics of carboxylate exchange result in a solution of oligomers which has a higher entropy of mixing.

Experimental Section

X-ray Diffraction Structure Determination and Refinement. Crystals of 2 and phases I and II of 1 were grown by slow crystallization from hot toluene. Compound 2 crystals were grown under Ar, the others in air. Phase III of 1 predominated when rapid crystallization was induced by addition of pentane to a saturated solution of 1 in toluene. All crystals were ~0.1–0.2 mm in size.

All crystals were sealed in glass capillaries in air, except 2 which was sealed under N_2. Data were collected using a Nicolet P3F automated single-crystal diffractometer and monochromated Mo Kα radiation. All data collection was performed at approximately −100 °C except for phase III of 1, which was performed at room temperature because these crystals repeatedly fractured upon cooling. Density measurements were not made. Each structure was solved by direct methods using the SHELXTL program package[14] on a Data General Eclipse S/140 computer. All hydrogen

Table XIII. Elemental Analysis Data

	anal. calcd		found	
compd	C	H	C	H
$[Bu_2Sn(O_2CCMe_2CO_2)]_x$ $C_{13}H_{24}SnO_4$	43.01	6.66	43.10	6.76
$[Bu_2Sn(O_2CCEt_2CO_2)]_x$ $C_{15}H_{28}SnO_4$	46.07	7.22	46.03	7.31
$[Bu_2Sn(O_2C(CH_2)_2CO_2)]_x$ $C_{12}H_{22}SnO_4$	41.30	6.36	41.05	6.31
$[Bu_2Sn(O_2CCH_2CMe_2CO_2)]_x$ $C_{14}H_{26}SnO_4$	44.60	6.95	44.41	7.17
$[Bu_2Sn(O_2C(CH_2)_3CO_2)]_x$ $C_{13}H_{24}SnO_4$	43.01	6.66	42.81	6.75
$[Bu_2Sn(O_2CCH_2CMe_2CH_2CO_2)]_x$ $C_{15}H_{28}SnO_4$	46.07	7.22	46.31	7.42
$[Bu_2Sn(O_2C(CH_2)_4CO_2)]_x$ $C_{14}H_{26}SnO_4$	44.60	6.95	44.56	7.19
$[Bu_2Sn(O_2C(CH_2)_8CO_2)]_x$ $C_{18}H_{34}SnO_4$	49.91	7.91	50.00	8.21
$[Bu_2Sn(O_2CC_6H_4CO_2)]_x$ $C_{16}H_{22}SnO_4$	48.40	5.59	48.69	5.74
$[Bu_2Sn(O_2CCEt_2CO_2)(H_2N(CH_2)_2NH(CH_2)_3Si(OMe)_3)]_x$ $C_{23}H_{50}N_2SnO_7Si$	45.03	8.22	45.08	8.37
$Bu_2Sn(O_2CCEt_2CO_2H)_2$ $C_{22}H_{40}SnO_8$	47.94	7.31	47.92	7.34
$Bu_2Sn(O_2CCH_2CMe_2CO_2H)$ $C_{20}H_{36}SnO_8$	45.91	6.94	45.44	7.00

positions were located using a difference Fourier synthesis and, in the final stages of refinement (on *F*), constrained to have appropriate bond lengths and angles. All non-hydrogen atoms were treated as anisotropic, except for phase III where the room temperature data did not warrant this. For this structure, only the Sn atoms were refined anisotropically. No absorption correction was performed for any of the structures, and no correction for secondary extinction was made. Details of the data collection for each of the structures is contained in Table X.

X-ray powder patterns were obtained using an automated Rigaku θ/θ diffractometer and monchromated Cu Kα radiation. Powders were packed in holders and run at room temperature in air. Simulations of the powder patterns from the single-crystal data were performed using the POWD7 program on a VAX 11/750 computer. Comparisons were performed graphically using SPECPLOT.

Crystallographic Summary. $[Bu_2Sn(diethylmalonato)]_x$—Phase I. $SnC_{15}H_{28}O_4$: M_r = 390.86, monoclinic, $P2_1/c$, a = 12.897 (6) Å, b = 10.530 (5) Å, c = 13.52 (1) Å, β = 108.38 (5)°, V = 1742.5 Å^3, Z = 4, D_x = 1.49 g/cm^3, Mo Kα, 0.71069 Å, $F(000)$ = 799.92, T = −100 °C, R = 0.0314 for 1991 unique observed reflections.

$[Bu_2Sn(diethylmalonato)]_x$—Phase II. $SnC_{15}H_{28}O_4$: M_r = 390.86, monoclinic, $P2_1/n$, a = 11.342 (2) Å, b = 11.677 (3) Å, c = 13.535 (4) Å, β = 108.64 (2)°, V = 1698.6 Å^3, Z = 4, D_x = 1.53 g/cm^3, Mo Kα, 0.71069 Å, $F(000)$ = 799.92, T = −100 °C, R = 0.0529 for 2327 unique observed reflections.

$[Bu_2Sn(diethylmalonato)]_x$—Phase III. $SnC_{15}H_{28}O_4$: M_r = 390.86, monoclinic, $P2_1$, a = 12.062 (6) Å, b = 11.188 (7) Å, c = 14.597 (6) Å, β = 114.38 (2)°, V = 1794.2 Å^3, Z = 2, D_x = 1.45 g/cm^3, Mo Kα, 0.71069 Å, $F(000)$ = 799.92, T = 25 °C, R = 0.0996 for 1417 unique observed reflections.

$[Bu_2Sn(diethylmalonato)((\gamma$-((aminoethyl)amino)propyl)trimethoxysilane)$]_x$. $SnC_{23}H_{50}O_7N_2Si$: M_r = 612.69, monoclinic, $P2_1/a$, a = 13.59 (1) Å, b = 13.06 (1) Å, c = 17.74 (2) Å, β = 106.15 (8)°, V = 3024.8 Å^3, Z = 4, D_x = 1.35 g/cm^3, Mo Kα, 0.71069 Å, $F(000)$ = 1279.83, T = −100 °C, R = 0.0560 for 3417 unique observed reflections.

NMR and MW Determination Parameters. ^{1}H NMR spectra were recorded at 300 MHz, ^{13}C NMR at 75.427 MHz, ^{29}Si NMR at 59.6 MHz, and ^{119}Sn NMR at 111.86 MHz on a Varian XL-300 spectrometer. All spectra were obtained in $CDCl_3$ solution, except where noted, and are referenced to Me_4Si or Me_4Sn (for ^{119}Sn NMR).

Vapor-phase osmometric molecular weight analyses (in $CHCl_3$) and elemental analyses were performed by Schwarzkopf Microanalytical Labs.

Preparation and Solution Characterization of $[Bu_2Sn(dicarboxylato)]_x$ Complexes. All reagents used in the synthesis of these complexes were purchased and used as received. These compounds were prepared by refluxing $[BuSn(O)]_x$ with 1 equiv of the appropriate dicarboxylic acid in toluene. The only exception was $[Bu_2Sn(phthalato)]_x$ which was prepared from phthallic anhydride. After the solutions became homogeneous (usually less than 1 h), the water was removed by azeotropic distillation into a Dean–Stark trap. The reaction mixtures were then filtered while hot, and solvent was removed in vacuo to give high yields (>95%) of $[Bu_2Sn(dicarboxylato)]_x$ as white crystalline solids. These products were then recrystallized from toluene/pentane or CH_2Cl_2/pentane. These compounds are not moisture sensitive.

Characterization was achieved using ^{1}H NMR, ^{13}C NMR,[15] ^{119}Sn NMR, vapor-phase osometric (VPO) molecular weight, IR (in $CHCl_3$), and C and H analysis. The ^{119}Sn NMR, IR, and VPO data are listed in Table IX, ^{1}H NMR data in Table XI, ^{13}C NMR data in Table XII, and elemental analysis data in Table XIII.

Preparation and Characterization of 2. Compound 2 is moisture sensitive and was prepared and handled under argon in a Vacuum Atmospheres HE 43-2 drybox. The diamine was purchased and distilled. Compound 1 (5.0 g, 12.8 mmol) and (γ-((aminoethyl)amino)propyl)trimethoxysilane (2.84 g, 12.8 mmol) were dissolved together in 10 mL of dry CH_2Cl_2. The solvent was removed in vacuo, yielding a pale yellow oil which crystallized after standing at 25 °C for several days. This product was recrystallized from CH_2Cl_2 at −30 °C giving 7.5 g (95%) of white crystals.

Preparation and Characterization of $Bu_2Sn(O_2CCEt_2CO_2H)_2$. $[Bu_2Sn(O)]_x$ (10.0 g, 40.2 mmol) and diethylmalonic acid (12.87 g, 80.4 mmol) were refluxed together in 100 mL of toluene. The solution became homogeneous after $^1/_2$ h, and the water was removed by azeotropic distillation into a Dean–Stark trap. The solvent was removed in vacuo and pentane was added to induce crystallization. White crystals were collected by filtration, washed with pentane, and dried in vacuo (21.0 g, 95% yield).

Preparation and Characterization of $Bu_2Sn(O_2CCH_2CMe_2CO_2H)_2$. This compound was prepared using the same experimental procedure as described above for $Bu_2Sn(O_2CCEt_2CO_2H)_2$ (yield = 85%).

Acknowledgment. We acknowledge Liz Williams, Joanne Smith, and Paul Donahue for NMR spectra; Steve Dorn for mass spectroscopy; Paul Schields and Don Marsh for powder pattern X-ray diffraction analyses; and Cathy Markowski and Pam Northrop for preparation of the manuscript.

Supplementary Material Available: Tables of all anisotropic thermal parameters and hydrogen coordinates for phases I, II, and III of 1 and for 2 (7 pages); listings of structure factors for phases I–III of 1 and for 2 (50 pages). Ordering information is given on any current masthead page.

---

(14) Sheldrick, G. M. *SHELXTL User Manual*; Siemens Analytical X-ray Instruments: Madison, WI, 1981.

(15) ^{13}C NMR assignments of the butyl Sn carbons were made by comparison with known compounds as described in: Mitchell, T. N. *J. Organomet. Chem.* **1973**, *59*, 189.